Supporting Information for:

Twin-Free Single-Crystal Ag Nanoplate Plasmonic Platform: Hybridization of Optical Nano-Antenna and Surface Plasmon Active Surface

Hyoban Lee,[†,&] *Kwang-Yong Jeong,*[‡,&] *Taejoon Kang,*[†,a] *Min-Kyo Seo,**[‡,§] *and Bongsoo Kim**[†,§]

[†]Department of Chemistry, KAIST, Daejeon 305-701, Korea

[‡]Department of Physics, KAIST, Daejeon 305-701, Korea

[a]BioNanotechnology Research Center, KRIBB, Daejeon 305-806, Korea

[§]KAIST Institute for the NanoCentury, KAIST, Daejeon 305-701, Korea

[&]These authors contributed equally to this work.

*E-mail: (M.-K.S.) minkyo_seo@kaist.ac.kr; (B.K.) bongsoo@kaist.ac.kr;

This supporting information includes Supplementary Figures S1 – S6.

Experimental Details

Synthesis of single-crystalline Ag nanoplates. We placed a Ag slug in an alumina boat at the middle of a 1 in. diameter horizontal quartz tube furnace (Figure S1). The Ag slug was heated to 820 ~ 840 °C and then carrier gas transports Ag vapor to the lower temperature region, where Ag nanoplates were grown on a $SrTiO_3$ (STO) (001) substrate. The distance from the center of a heating zone to the substrate was 5 cm and Ar gas flowed at a rate of 100 sccm, maintaining the chamber pressure of 2 ~ 5 torr.

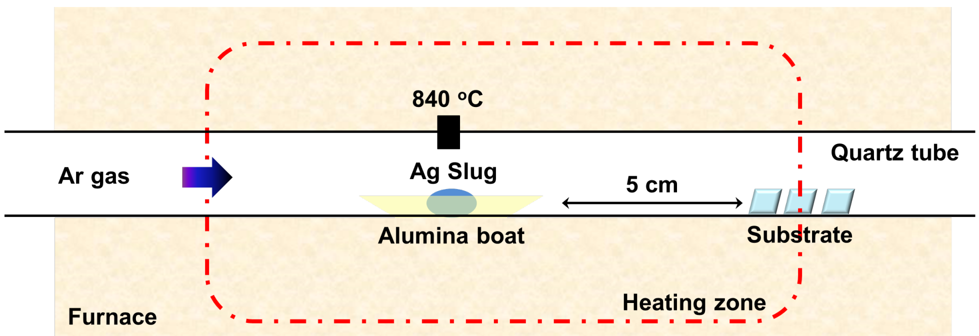

Supplementary Figure S1. Schematic of the horizontal quartz tube furnace system for the synthesis of Ag nanoplate.

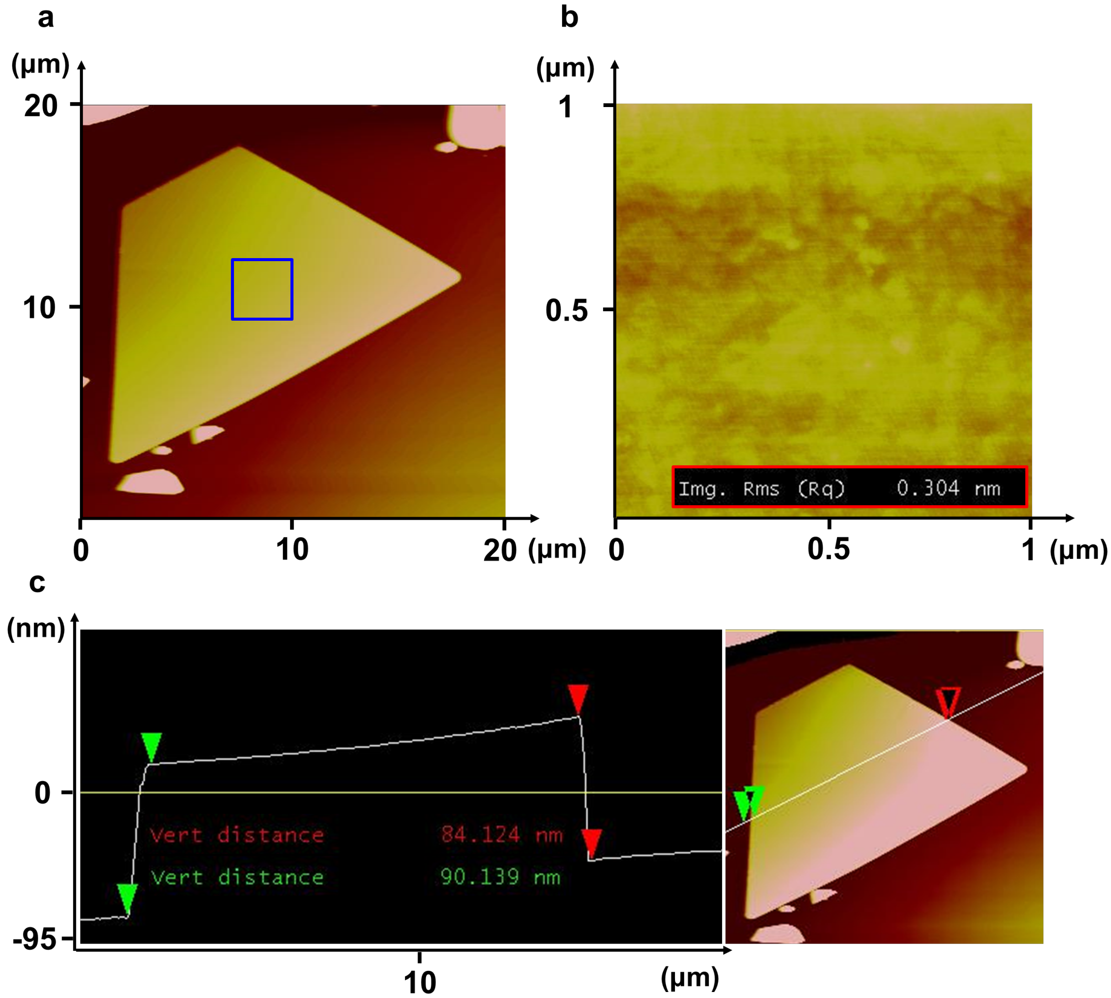

Supplementary Figure S2. Atomic force microscope (AFM) analysis for as-synthesized Ag nanoplate. (a) Low-resolution image of isosceles-trapezoid shaped hexagon Ag nanoplate. (b) Magnified image for blue box in (a). Root-mean-square (rms) roughness is 0.304 nm as shown as red-box, indicating that our Ag nanoplate has atomically smooth surface. (c) Sectional analysis result shows the thickness of Ag nanoplate is ~ 90 nm.

Simulated incoupling efficiency of normal incident light at the nanoplate side. We performed 3D FDTD simulations employing a semi-infinite Ag nanoplate and a focused Gaussian beam with a spot size of 500 nm. First, we calculated the flux of SPPs (P_{SPP}) along the nanoplate and the total flux of the incident light ($P_{incidence}$) respectively. The fractions of $P_{SPP}/P_{incidence}$ were plotted as a function of the distance from the input antenna side (black dots). By fitting the plot for the range from 2 to 3 μm (red line), the in-coupling efficiency can be estimated from the extrapolated value of the red line at the distance of zero, which is ~5.9%. The difference between the black dots and red curve at the short distance range is due to the direct reflection of the incident light.

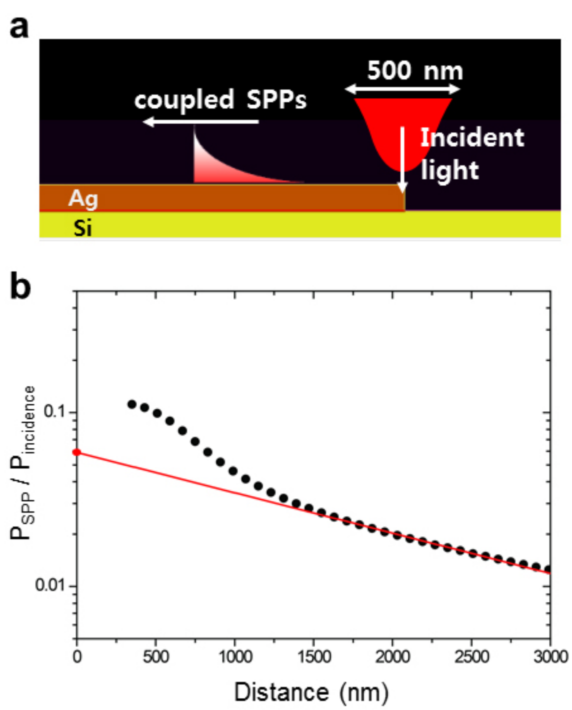

Supplementary Figure S3. (a) Schematics of the in-coupling simulation showing a focused incident light and the propagating SPPs coupled at the nanoplate side. (b) Fraction of power coupled to SPPs along the nanoplate.

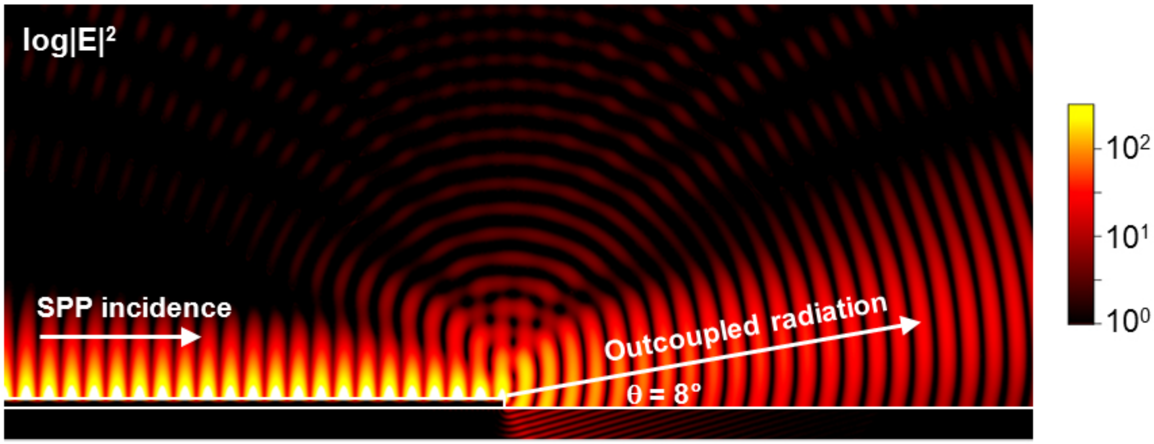

Supplementary Figure S4. Out-coupling of SPPs to free-space radiation at the Ag nanoplate side. Side-view of the simulated electric field intensity shows that out-coupled radiation from the nanoplate side is propagating at an angle of ~8° with respect to the nanoplate plane. The total power of radiation to the top air free-space is calculated to be ~32%.

Transmission and reflection coefficients of SPPs across a nano-gap. We performed 2D FDTD simulations and calculated the transmitted and reflected powers of SPPs across the nano-gap. When the gap is 90 nm as same as the experiment, the transmission of SPPs is ~57%. The fluctuations of the efficiencies are resulted from phase matching conditions depending on the gap width and the SPP wavelength.

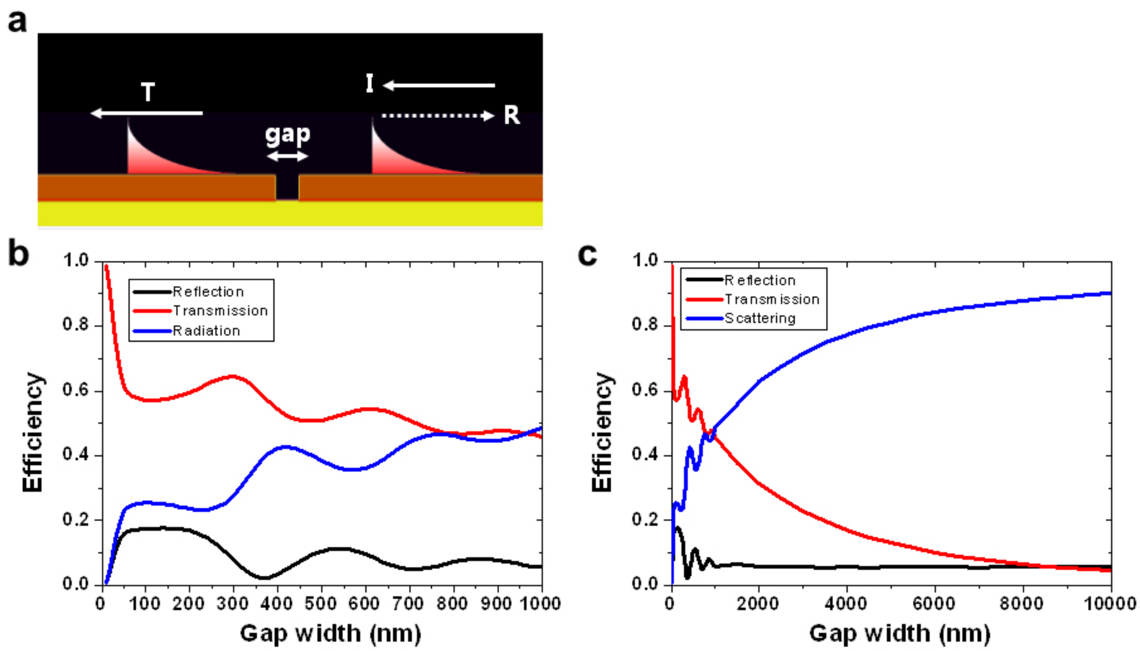

Supplementary Figure S5. (a) Schematics of the simulation of reflection and transmission coefficients of SPPs across a nano-gap introduced in the Ag nanoplate. (b, c) Fraction of power transmitted across the nano-gap (black line), reflected back (red line), and scattered (blue line) as a function of the gap size.

Blocking SPP propagation by a dust scatterer. In contrast to a metallic nano-belt (Figure 4) or a nano-gap (Figure 5), the dust completely blocks propagation of SPPs generated by the incident laser light. It is clearly observed that SPPs scattered by the dust radiate with a polarization state parallel to the propagation direction (or perpendicular to the input side).

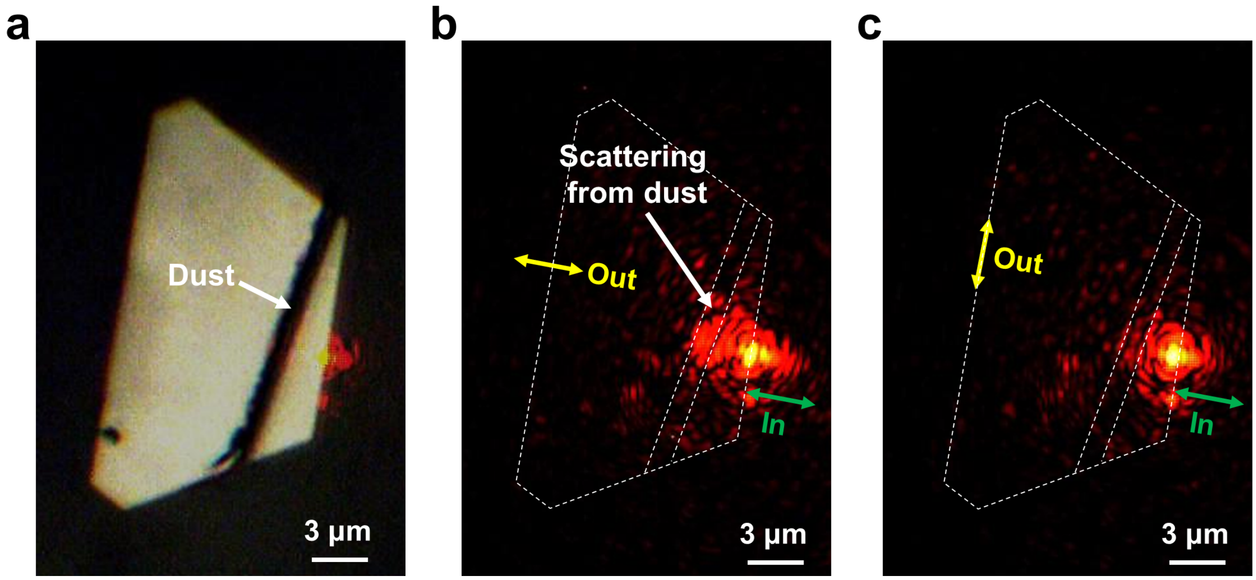

Supplementary Figure S6. (a) An optical microscopy image of a Ag nanoplate involving a solid dust on its surface. (b,c) Polarization-resolved measurements of radiation distribution on the Ag nanoplate. Dashed lines indicate the outline of Ag nanoplate and a solid dust.